Indian Journal of Chemistry
Vol. 63, February 2024, pp. 211-225
DOI: 10.56042/ijc.v63i2.3515

Facile synthesis, spectral characterization and biological evaluation of metal complexes comprising ((1-hydroxynaphthalen-2-yl) methyleneamino-cyclohexylimino-methyl)naphthalen-1-ol Schiff base ligand and assessing chemo pharmaceutical properties

J Priya, S Manimalathi & D Madheswari*

Government Arts College for Women, Salem 636 008, Tamil Nadu, India

E-mail: drmadhu6666@yahoo.com

Received 1 July 2023; accepted (revised) 18 January 2024

This work particularize a series of transition metal complexes such as Mn, Fe, Co, Ni, Cu and Zn, which have been synthesized from newly synthesized bidentate Schiff base ligand namely ((1-hydroxynaphthalen-2-yl)methyleneamino-cyclohexylimino-methyl)-naphthalen-1-ol and anticipated to evaluate the chemopharmaceutical properties of metal complexes. The Schiff base ligand and corresponding transition metal complexes have been characterized by spectral studies such as elemental analysis, UV-Vis, FT-IR, ^{1}H NMR, ^{13}C NMR spectroscopy and ESI mass spectrometry. Schiff base metal complexes have been screened for their *in-vitro* antimicrobial activities against bacterial and fungal strains in order to prove their biological activity. The theoretical molecular docking studies revealed the existence of favorable interaction between biomolecule and synthesized complexes. Outcome of the investigation proved that the transition metal complexes exhibited prominent activity towards MCF17 breast cancer tumor cell lines and therefore appropriate to design new therapeutic chemopharmaceuticals with vital applicability and good values of antiproliferative activity.

Keywords: Antiproliferative activity, Antimicrobial activity, Chemopharmaceuticals, Molecular docking, Schiff base

Undoubtedly, design and development of metallopharmaceuticals remains one of the major research exploration for the past few decades, as they are used mainly for chemotherapic treatment to combat tumour[1-4]. Even though platinum-based metallo pharmaceuticals have significant advantage as an anticancer drug, the current situation calls for other substances with more specific activity, which are able to distinguish between different types of cancer, as well as more selective, competent of identifying between cancer cells and healthy cells. Along this route, researchers focused more on coordination complexes, namely metal compounds produced from Schiff base ligands. The azomethine group (>C=N linkage imine bond) is present in the chemical makeup of Schiff bases, which are derived from the environment and play important roles in a variety of biological developments. This group is created by the condensation of an amine and a carbonyl group, which results in the formation of a hemiaminal group[5-9]. The results of the work include the exploration of numerous metals from the periodic table, mainly from the d-block, as well as a variety of organic ligands, preferably with demonstrated bioactivities[10]. As a result of their readily available basic components, ideal synthesis conditions, and controllable density, Schiff bases have been shown in numerous studies to be effective binders.

The unique chemical constitution encompassing azomethine group possess excellent biological, catalytic, thermal and electrochemical properties that are widely applicable for food industry, dye industry, analytical chemistry, catalysis, fungicidal, agrochemical industry. Expressly, the antimicrobial[11], anticancer[12], antitumor[13], antioxidant[14], anti-inflammatory[15], antiviral[16], and herbicidal[17] activities. Due to the rising interest in using metal compounds made from Schiff bases to treat cancer, our literature review was motivated by this topic principally[18-28].

Curiously, hydroxyl naphthalene-derived Schiff base ligands have been studied earlier and proven to exhibit remarkable biological activity that may form stable complexes with a range of transition metals. As a result, transition metal complexes with Schiff base ligands generated from hydroxyl naphthalene are increasingly being used medicinally. A literature

review finds that some coordination complexes generated from Schiff bases that have previously shown biological activity now have anticancer activity. This is because the structure of the ligand has a significant impact. Additionally, adding functional groups to specific Schiff base positions makes the base more cytotoxic. Our earlier investigations evidenced that the stronger antiproliferative activity of salicylaldehyde-based Schiff base nickel complex that has been originated from the unique ligand structure[29,30].

Herein, we intended to explore a Schiff base produced by the condensation of 1-hydroxy-2-naphthaldehyde and cyclohexane-1,2-diamine since the type of ligands has a significant impact on biological characteristics as well as binding and cleaving capabilities with biomolecules that greatly influence the antiproliferative (cytotoxic) properties. Schiff base ligands, specifically the halo-salicylaldehyde moiety, have been shown as chemotherapeutic agents against several cell types. Two-hydroxy-1-naphthaldehyde and 5-chloro-2-hydroxybenzoylhydrazone are included in a series of new organotin complexes that have been synthesized and shown to have good *in vitro* antitumor activity against human colon cancer cells (HCT-8), lung cancer cells (A549), and human promyelocytic leukemic cells (HL-60)[31]. Also, mononuclear complexes of Schiff base ligand synthesized from 2-hydroxy-1-naphthaldehyde and 2-methoxyethylamine was shown to be inhibitory towards the growth of MKN-45 cancer cell line[32]. Copper and nickel complexes with Schiff base, which are made from 2-hydroxy-1-naphthaldehyde-4-aminoantipyrine Schiff-base, have recently been shown to have good anticancer properties by Qi et al[33]. Besides, Cd(II), Zn(II) and Co(II) complexes with Schiff base encompassing thiazole and 2-hydroxy-1-naphthaldehyde showed good cytotoxic property along with good DNA cleaving ability[34]. 2-hydroxy-1-naphthaldehyde Schiff-base ligand derived nickel ternary complex was investigated theoretically for pharmaceutical potential and was demonstrated for drug-likeness parameters[35]. The literature survey clearly proved that 2-hydroxy-1-naphthaldehyde based ligand has a potential to form anticancer molecules. Therefore, our present work planned to synthesize new Schiff base ligand, by the condensation of 3-hydroxy-2-naphthaldehyde with cyclohexane-1,2-diamine and its transition metal complex with Mn(II), Fe(II), Co(II), Ni(II), Cu(II), Zn(II), Cd(II) and Pb(II) were characterized by using spectroscopic techniques. Next, the synthesized transition metal complex were subjected to antifungal assay against *Candida albicans and Aspergillus niger*. The anticancer activity of the Schiff base ligand and its complexes was investigated against cytotoxic action against human breast cancer MCF-7 cells.

Following this line of examination, we established a straightforward process for the synthesis of a novel Schiff ligand derived from, 2-hydroxy-1-naphthaldehyde and cyclohexane-1, 2-diamine, as well as a number of new transition metal complexes. For the produced metal complexes, spectroscopic and biological investigations are conducted to understand their pharmacological action. In addition, we have conducted anticancer experiments on Nickel metal complex as a model chemical. This research has generated information on the chemicals' powerful usage in anticancer treatment.

Experimental Section

All the reagents and solvents were purchased from Loba Chem. Ltd, Merck, and used without further purification. TLC was performed on Merck pre-coated aluminum sheet of 60 F-254 silica gel plates using hexane/ethyl acetate as solvent system for the mobile phase with UV and Visible light and also with iodine spray. Melting points were measured using a Buchi Melting point B-545, an electro thermal apparatus using capillary tubes which are uncorrected. ^{1}H NMR and ^{13}C NMR spectra were recorded on a Bruker 400 MHz or 100 MHz high resolution NMR spectrometer respectively and proton chemical shifts (δ) are referenced to the solvent (DMSO-d_6 at 2.51 ppm). FT-IR spectra were recorded on a Bruker FT-IR27 spectrometer using KBr disks. The mass spectra were recorded on an Agilent 6520 Q-TOF spectrometer. Organic solvents were reagent grade. The antibiotic was purchased from Egyptian markets and used as standard for antifungal activities.

Synthesis of ligand

((1-hydroxynaphthalen-2-yl)methyleneamino-cyclohexylimino) methyl- naphthalen-1-ol was prepared by mixing 2 mmol of 3-hydroxy-2-naphthaldehyde and 1 mmol of cyclohexane-1,2-diamine in ethanol stirred at room temperature. The reaction was monitored by TLC using hexane/ethyl acetate (7:3) mobile phase within 30 minutes until complete disappearance of the starting material. After completion of the reaction, the solid product was separated by filtration technique, washed thoroughly with ethanol and deionized water, dried at 60^{o}C, and stored for further studies.

Synthesis of Schiff base transition metal complexes

The metal complexes were synthesized by the addition of 5 ml of ethanolic solution of methylacetate/citrate (1 mmol) and Schiff base ligand (1 mmol) in a round bottom flask. The reaction mixture was stirred at a reflux condition for an appropriate reaction time and the solid metal complex was cooled to room temperature. The obtained metal complex was filtered, dried at 60ºC.

Table 1 denotes proposed molecular structure and molecular formula for the synthesised ligand and metal complexes.

Table 1 — Proposed Molecular Structure and Molecular Formula for the Synthesised Ligand and Metal Complexes

Entry	Ligand/complex	Molecular formula	Molecular Weight	Time (min)	Colour	Yield (%)
1	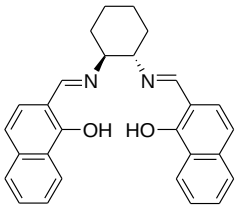 Ligand (A)	$C_{28}H_{26}N_2O_2$	422.52	30	Pale yellow	98
2	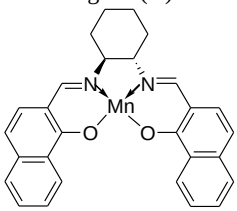 B	$C_{28}H_{24}MnN_2O_2$	475.44	90	Deep Brown	85
3	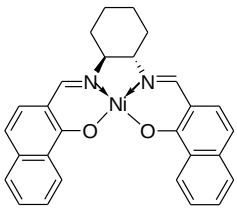 C	$C_{28}H_{24}NiN_2O_2$	479.2	90	Orange	68
4	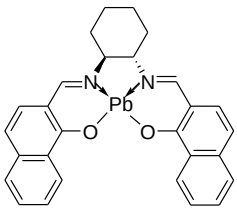 D	$C_{28}H_{24}N_2O_2Pb$	627.7	90	Pale brown	89
5	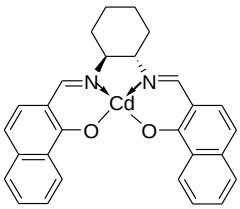 E	$C_{28}H_{24}CdN_2O_2$	532.91		Black	95
6	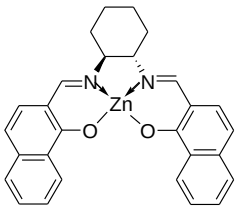 F	$C_{28}H_{24}N_2O_2Zn$	485.89		Black	89

Microbial cultures

The fungal strain such as *Aspergillus niger* and *Candida albicans* were used throughout investigation. All the fungal cultures were obtained from Microbial Type Culture Collection (MTCC), Institute of Microbial Technology and Chandigarh, India. The young fungal broth cultures were prepared before the screening procedure.

Antibacterial Activity

Antibacterial activity of synthesized ligand and metal complexes are tested by viable count technique against Escherichia coli and Staphylococcus aureus as a model bacteria. For this investigation, 108 colony forming units (CFU) of individual bacterium are grown in 10 ml nutrient broth supplement with film discs (15 mm diameter). The bacterial viability is determined using their optical density values by UV-Vis spectroscopy[36,37].

Antifungal activity

The synthesized Schiff base ligand and its transition metal complexes were screened for the antifungal activity tested against two fungal species like *Candida albicans and Aspergillus niger* using agar well diffusion method[38] by measuring the inhibition zone in mm. Fungal culture were grown in a Sabouraud's dextrose broth at 37 ºC for 6 h under laboratory condition. The sterilized agar media poured into Petri-dishes and allowed to solidify. On the surface of the media, fungal suspension was spread with the help of sterilized triangular loop. A stainless steel cylinder of 10 mm diameter (pre-sterilized) was used to bore cavities. All the transition metal complexes and its ligand were placed serially in the cavities with the help of micropipette and allowed to diffuse for 1h, the transition metal complexes and ligand were dissolved in DMSO. These plates were incubated at 37ºC for 72 h for antifungal activities. The zone of inhibition observed in the respective incubation was measured. Fucanazole (1 mg/mL) was used as a standard drug for antifungal activity.

DPPH anti-oxidant studies

A Shimadzu modell UV-1601 spectrophotometer was used to measure the antioxidant activity. As a stable free radical, 1,1-diphenyl-2-picryl-hydrazyl (DPPH), which is red, was used. The mixes were created by adding predetermined amounts of DPPH (0.1 mM) to ethanol solutions at concentrations of 10, 20, 30, and 40 g/mL. At room temperature, inhibition lasted for 20 minutes, and 517 nm absorbance was calculated. The standard used was ascorbic acid. If DPPH produces free radicals, its red colour turns yellow. Following is how the inhibitory level of DPPH was determined[39].

$$\text{DPPH scavenging (\%)} = (A_0 - A_{sample}/A_0) \times 100 \quad \ldots (1)$$

where, A_{sample} is the sample's absorbance and A_0 is the absorbance of the control. For L and the complexes, IC50 values were computed. The concentration needed to achieve 50% of the maximum scavenging activity is known as the IC50 value.

Molecular Docking of compounds

Chem Draw 12.0 was used to draw the chemical structures of the synthesized ligand and metal complexes in particular, and the structures were saved in Mol file format. The Mol files of compounds were then converted into PDB (protein data bank) format using open babel. For molecular docking analysis, the human Bcl-2 (PDB ID: 1GJH) isoform were retrieved from the database PDB (protein databank). The structure of human Bcl-2 was published in the article by Petros et al.[40]. The molecular docking was accomplished to investigate the binding mode of compounds A-F and curcumin with human Bcl-2 isoform. Docking study for 4k and 6f was performed using a Patch Dock online server[41]. The clustering RMSD was 4.0 Å and the complex type was set to default. The number of solutions with their score, area, and desolvation energy were obtained. Patch Dock provided results, that were ranked according to geometric shape complementarily score after molecular shape representation and surface patch matching. Further, the Discovery Studio 4.0 Client was used for visualization and determining the mode of interaction between the receptor and ligands[42].

Anticancer studies

Cell Culture Maintenance

MCF7 breast epithelial adenocarcinoma cancer cell line was obtained from the National Centre for Cell Sciences (NCCS), Pune, India. Cells was maintained in the logarithmic phase of growth in DMEM medium supplemented with 10% (v/v) heat inactivated fetal bovine serum, 100 U/ml penicillin, 100 µg/ml streptomycin. It was maintained at 37°C with 5% CO_2 - 95% air humidified incubator.

Cytotoxicity of Cell Lines (MTT) Assay

The cytotoxic effect of complex 4b tested against cancer cell lines such as MCF7 by MTT (3-(4, 5-

dimethylthiazol-2-yl)-2, 5-diphenyltetrazolium bromide) assay (Mossmann, 1983 and Md et al., 2020). Briefly, the cell lines were separately seeded in 96-well microplates (1×10^6 cells/ml) and incubated at 37°C for 24 h with 5% CO_2 incubator and allowed them to grow to 90% confluence. At end of the incubation, the medium was replaced and the metal complex 4b at different concentrations of 25, 50, 75, 100 and 150 µg/ml. Then the samples were incubated for 24 h. The cells were then washed with phosphate-buffered saline (PBS, *p*H -7.4) and added 20 µl of (MTT) solution (5 mg/ml) to each well and allowed to stand at 37°C in the dark for additional 4 h. Then added 100 µl DMSO and dissolved the form azan crystals and it absorbance was read spectrophotometry at 570 nm using ELISA plate reader. The percentage of cell viability was expressed as [42],

$$Cell\ Viability\ (\%) \frac{Absorbance\ of\ treated\ cells}{Absorbance\ of\ control} \text{ x } 100 \quad \ldots (2)$$

Statistical Analysis

All the grouped data were evaluated using PASW statistics 18 software. Hypothesis testing method included One-way analysis of variance (ANOVA) followed by significant difference tests. The p – value (p<0.05) was considered to indicate statistical significance. All the results were expressed as mean ± standard deviation (SD) for each test.

Results and Discussion

The Schiff base was synthesized by the condensation of 1-hydroxy 2-naphthaldehyde cyclohexane-1,2-diamine in a molar ratio of 2:1, after that it was complexed by direct reaction between Schiff base and transition metal chlorides/metal acetates to provide B-F as depicted in Scheme 1. The entire synthesized complexes are fairly stable and characterized by using FT-IR, UV, ^{1}H NMR, ^{13}C NMR and Mass spectroscopic techniques.

FT-IR spectra

The FT-IR spectra of ligand and metal complexes are as shown in Fig. 1, and they generally give information on the functional group of the derivative, coordination mode, and restricting sites of the ligand-to-metal ion. The infrared spectra of the metal-free ligand show absorption bands in the region 1629 cm^{-1} and can be assigned to C=N– of azomethine group. It is important to note, however, that the extent of the frequency shift was affected by the type of both the transition metal ion and the ligand involved in chelation. This is most likely owing to a shift in the electrostatic field of the metal ions as well as the ligand's vibrational dipoles. The complex formation with metal ion brings down the electronic density associated with azomethine group and therefore lowers the absorption frequency.

This bands shifted towards lower frequency when metal complexes are formed, showing that the coordination bonding has been created. In addition, the emergence of the Schiff base's phenolic hydroxyl group at 3533 cm^{-1}, which is displaced to 3428 cm^{-1}, 3435 cm^{-1}, 3554 cm^{-1}, 3389 cm^{-1}, and 3554 cm^{-1}, indicates that the coordination of phenolic oxygen has been involved in the co-ordination of metal ions. The new bonds appearing in the region of 500-600 cm^{-1} in spectra of all metal complexes demonstrate the formation of metal-nitrogen and metal-oxygen bonds that approve coordinate bonding sites.

Electronic spectra

The electronic transition spectra for all the new complexes and ligand have been recorded in DMSO solvent in the region 800–200 nm as shown in Fig. 2. UV spectra of free ligand shows two occasion groups in the locale of 260 nm, 330 nm and 430 nm due to $\pi \rightarrow \pi^*$ and $n \rightarrow \pi^*$ changes separately. The coordination of the free ligand to the metal ion may be responsible for the minimal height or growth observed in these frequencies. Metal Schiff base complexes show three to four bands in the visible and ultraviolet region 460–208 nm. The absorption spectra of Schiff base complexes in the high-intensity bandsin the region 208–260 nm that are very analogous and are attributable to the ligand–centered transitions

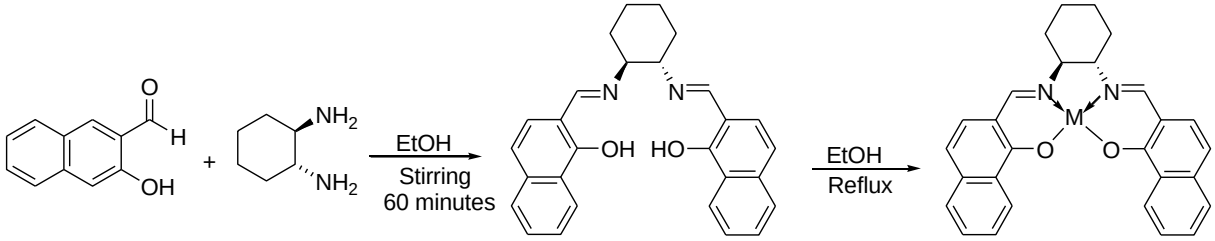

Scheme 1 — Synthesis of Schiff complex and transition metal complexes

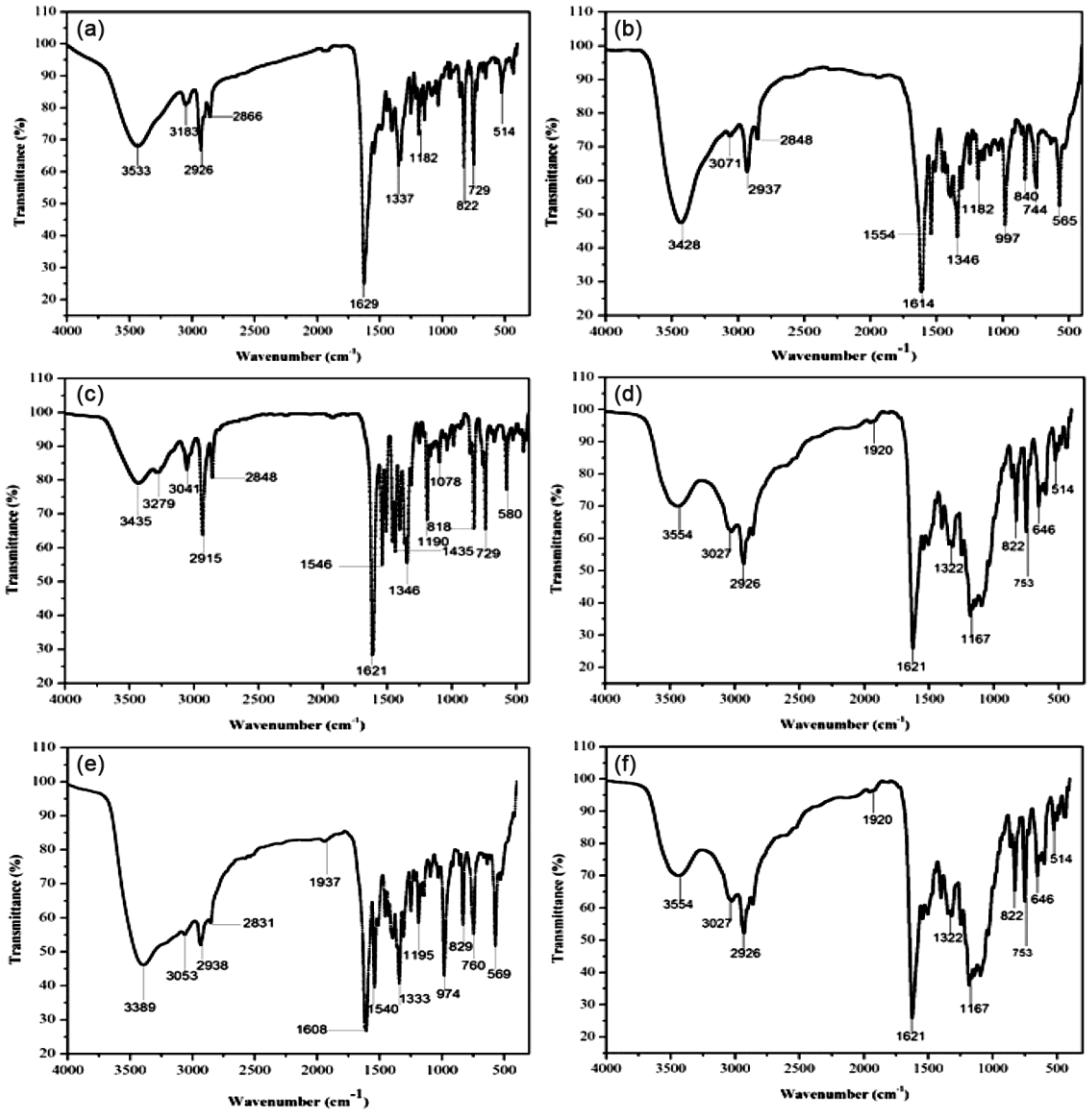

Fig. 1 — FTIR spectra of ligand as well as metal complexes.

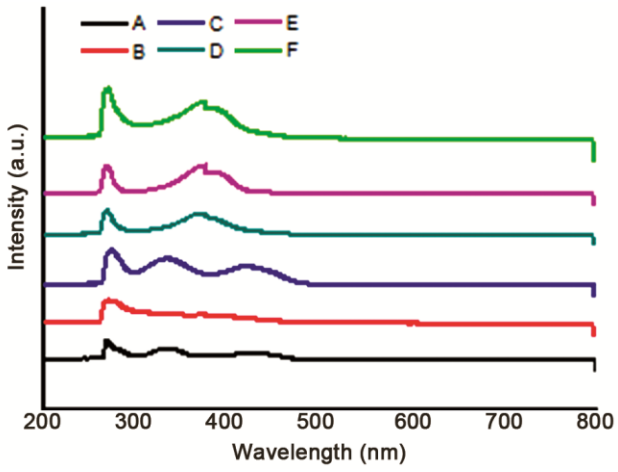

Fig. 2 — Electronic spectra of ligand and metal complexes.

(π–π*, n–π*) taking place in the aromatic group of Schiff base ligands. Complex B displays a broad band at 530 nm, which is predicted to be caused by the Mn(II) ion's d-d progress (2Eg 2T2g). This d-d change band insistently helps the octahedral structure around the metal ion sites. It has the attractive second estimation of 1.84 BM magnetic moment value to the uncoupled nature of the metal particle. Due to the metal to ligand charge transfer transitions, the lowest energy absorption bands emerged in the electronic spectra of the complexes. While complex C exhibits retention groups at wavelengths of 285 nm and 420 nm, respectively, that correspond to the electronic targets 4T1g (F) 4T2g (F) and 4T1g (F) 4T2g (P), and it has a magnetic moment value of 4.64 BM with an

octahedral geometry around the metal ion. In contrast to complex E, which does not exhibit any d-d transition, complex D exhibits d-d groups at 520 nm and 630 nm for the 3A2g (F) 3T 1g (F) and 3A 2g (F) 3T 1g (P) ranges, respectively. The complex H displays high intensity bands due to intramolecular ligand transition as well as charge transfer from ligand to metal.

NMR Spectra

To validate the findings, ^{1}H- NMR and ^{13}C- NMR spectra of ligand were collected, as shown in Fig. 3. In DMSO-d6, the ^{1}H- NMR spectra of Schiff base ligand were observed. The ligand's ^{1}H- NMR spectra displays a singlet at 14.3 ppm, indicating the presence of a hydroxyl proton on the aromatic ring. The presence of aromatic protons caused the peaks to form around 8.13-7.22 ppm. The singlet then occurred at 3.31 ppm, indicating a cyclohexane ring CH proton. The existence of cyclohexane ring methylene protons is indicated by the appearance of a signal at 1.93-1.09 ppm. Peaks at 163.24 ppm and 157.77 ppm in the ^{13}C- NMR spectra of the ligand show the existence of a C-OH group, whereas peaks at 137.73 to 109.72 ppm indicate the presence of aromatic carbon. The existence of cyclohexane ring carbon is also indicated by the remaining peaks. These observations substantiated the development of the suggested ligand structure.

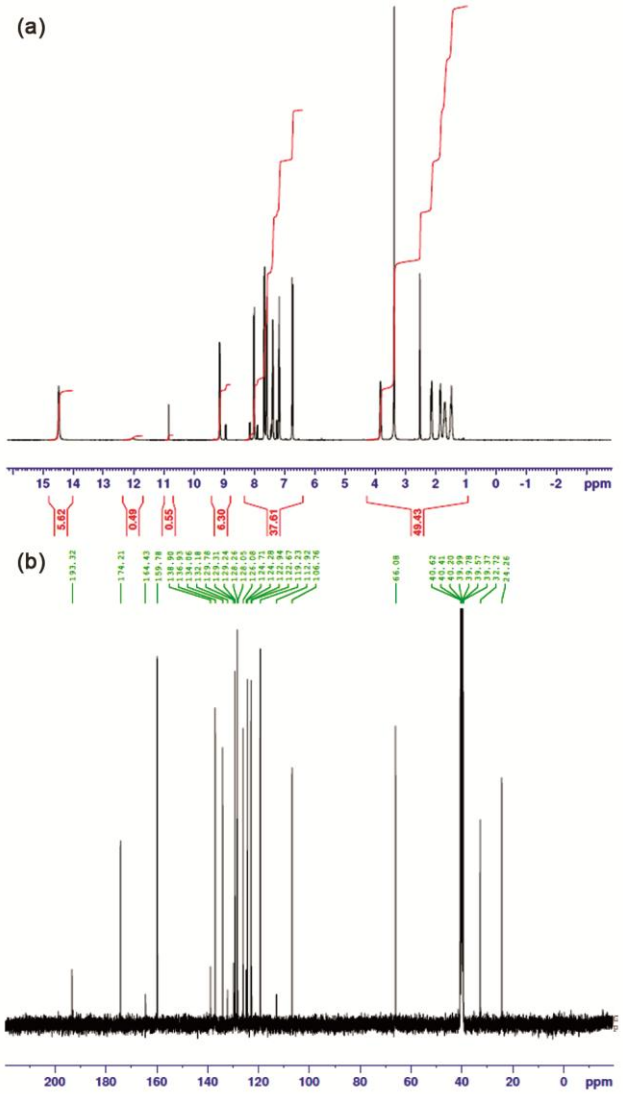

Fig. 3 — (a) ^{1}H-NMR and (b) ^{13}C-NMR spectra of ligand.

ESI Mass spectra

The molar mass and chemical makeup of substances can be ascertained by the use of mass spectrometry. The mass spectrum shows fragmentation of the target molecule through a series of peaks that represent the many pieces. The intensity displays the stability of the Schiff base fragments and metal complexes. The ESI-MS spectra show that ligands were synthesized by condensation. The ESI-MS spectra of the ligand is shown in Fig. 4. The ligand (L) has a significant mass peak around m/z 423. It suggests that the M+1 peak, which has the suggested chemical formula $C_{28}H_{26}N_2O_2$, has formed. The 1:1 ligand peak is indicated by the fragment peaks at 424 m/z. To confirm the postulated formula mass, the mass spectra of ligand as well as molecular ion peaks, was used.

Elemental analysis

Elemental analysis of the ligand and its transition metal complexes (B-F) are provided in Table 2, that displays the base ligand's percentage data for the elements carbon, hydrogen, and nitrogen (CHN), together with its matching metal (II) complexes. The experimental percentage is compared with calculated theoretical values, and we have determined a small deviation (±0.03-0.06) that falls within acceptable limit.

SEM and EDAX studies

The morphology of synthesized ligand (A) and its metal complex (F) were characterized by SEM analysis. The SEM images of A and F are represented in Fig. 5 and Fig. 6 respectively. The ligand displayed needle-like structural features that show distribution of agglomerated small grains in non-uniform shape and dimension as depicted in Fig. 5. However, distinctly different morphology is exhibited by complex F as shown in Fig. 6 that comprises regular shaped grains with elongated morphology without entangled pores as uniform lamellar grains.

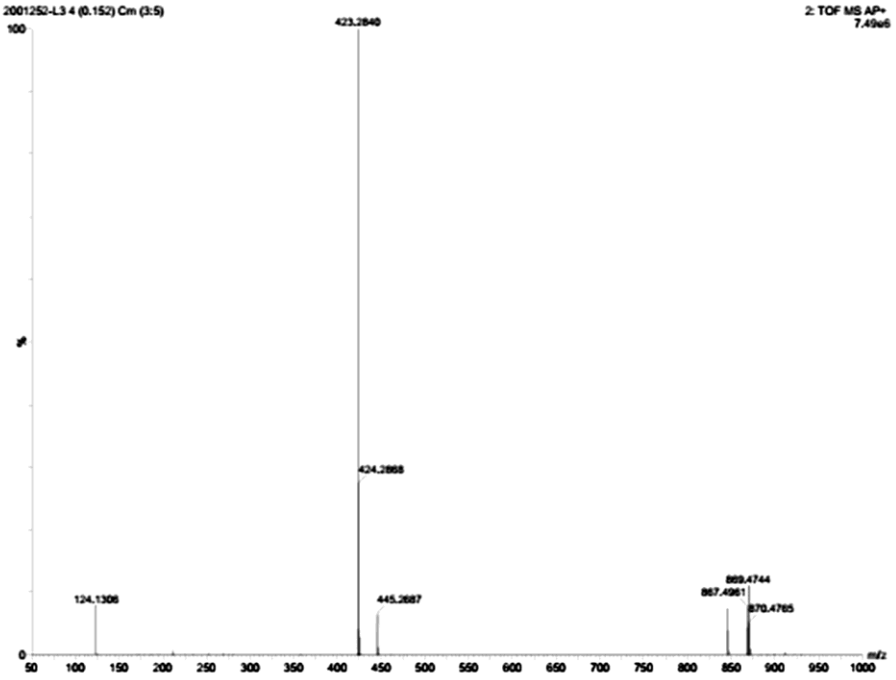

Fig. 4 — The mass spectra of Ligand.

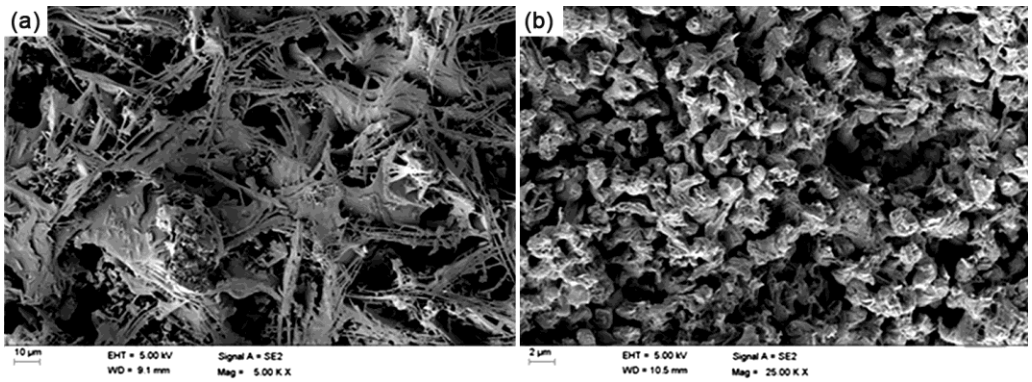

Fig. 5 — SEM images of (a,b) Ligand **.**

Table 2 — Calculated Elemental composition

S.No	Sample	Elemental composition [calculated] (%)		
		Carbon	Hydrogen	Oxygen
1	A	47.65 [46.98]	2.84 [2.90]	6.45 [6.89]
2	B	44.67 [43.49]	2.62 [2.22]	5.62 [5.43]
3	C	43.62 [44.09]	2.15 [2.12]	4.65 [4.30]
4	D	45.67 [45.07]	2.64 [2.87]	5.02 [4.98]
5	E	45.51 [44.87]	2.09 [1.89]	4.78 [4.45]
6	F	46.78 [46.09]	2.45 [2.54]	5.23 [5.09]

Thermal Analysis

The thermo-gravimetric analysis of synthesized ligand (A) and zinc metal complex (F) have been studied using TGA analysis as represented by Fig 7. The data show that the heat breakdown happens in 3 successive steps, step-by-step. Although, both ligand and complex F followed a similar degradation pattern, it is noteworthy that thermal decomposition rate is higher for ligand than complex F. At initial stage at the temperature below 100-120^{o} C, minimum weight-loss that has been associated with loss of solvent molecules is observed for both. And nearly 4% of water molecules have been excluded at this stage of degradation.

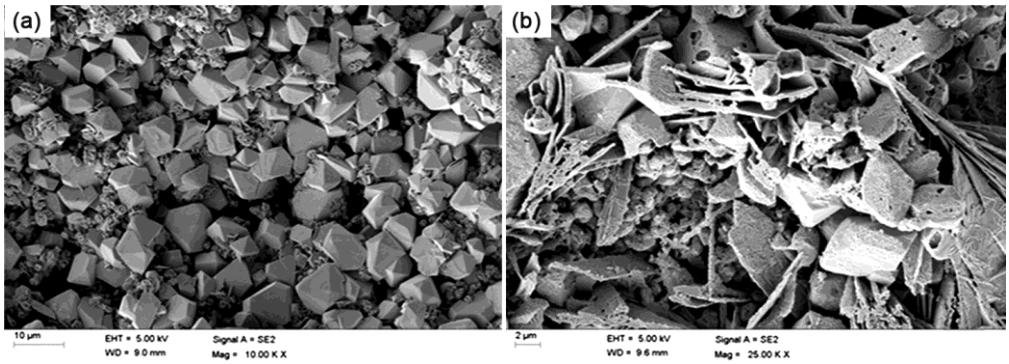

Fig. 6 — SEM images of (a,b) metal complex **F.**

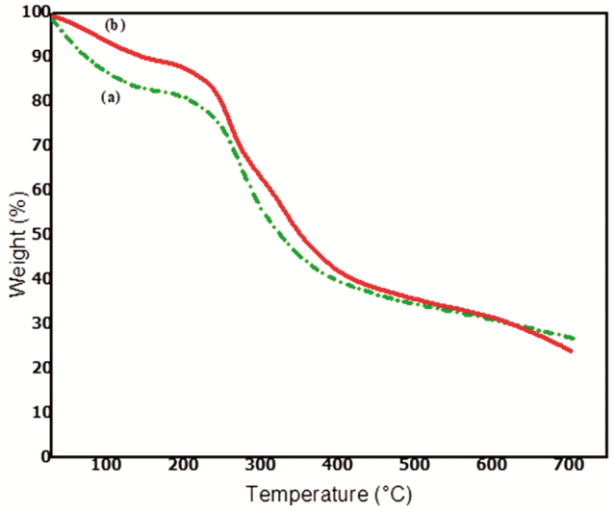

Fig. 7 — TGA graph of synthesized ligand and metal complex **F**.

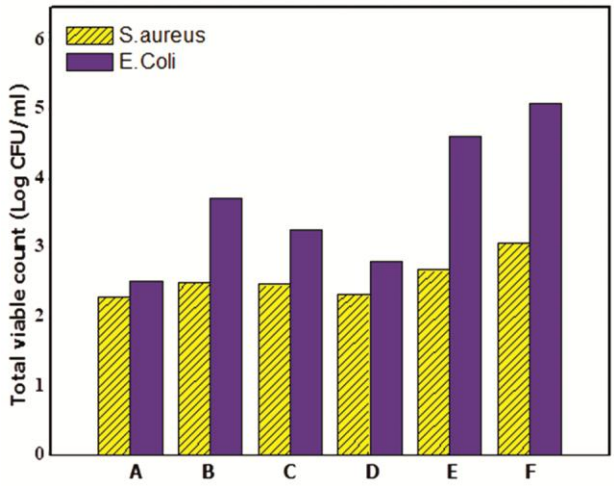

Fig. 8 — The antibacterial activity of the ligand and metal complexes measured by viable count method against *E.coli* and *S.aureus* bacterial strains.

The second stage weight loss has occurred beyond 200°C for metal complex **f,** however the ligand gets decomposed at this temperature. Between 190 and 230°C, the second stage of weight loss brought on by the cleavage of the metal-ligand link and partial ligand breakdown is noticed. At this point, the ligand began to break down, while complex F maintained stability despite losing about 25% of its weight. The main and last stage of weight loss occurs for the ligand above 270°C, whereas metal complex F is stable up to 400°C. The disintegration of ligand accompanied with structural decomposition happens at the elevated temperature and remaining weight exist as metallic oxide. The final deposit left encompassing metal oxide is ascribed due to ultimate collapse of metal complex occurred above 450°C. These studies proved that thermal properties have been reformed after metal complex formation and thermal stability of metal complex is higher as compared to ligand.

Biological Activity studies

Microbicidal property of synthesized ligand and metal complexes have been assessed by carrying out screening against bacterial and fungal strains that represent essential characteristics for functioning as medication and drugs. In general, metal chelates have been shown to have higher microbiological resistance than free ligands. Two bacterial strains were tested namely *S. aureus* and *E. coli* and the results are as shown in Fig. 8. The maximum activity was showed by complex F against *E. coli.* More specifically, following chelation with metal ions, the medications are more efficacious than free commercial organic pharmaceuticals. The results exposed that the metal complexes showed greater antibacterial activities in relation to the ligand.

Antibacterial activity

Antibacterial activity is one of the key necessities for better-performing chemotherapeutic agents. Fig. 8

represents anti-bacterial results of ligand and metal complexes **(B-F)** determined by viable count method. It is apparent that metal complex exhibit greater efficiency as compared to ligand against both *E. coli* and *S. aureus* bacterial strains. The metal complexes namely B, D and F presented superior activity against *E. coli*, while complex **C** and **D** displayed only average activity. Generally, both the ligand L and metal complexes B-F demonstrated improved inhibition against growth rate of *E. coli* as compared to *S. aureus* bacterial strain. It is noteworthy that, complex F presented greater inhibition activity towards the growth of both *E. coli* and *S. aureus.*

The antibacterial activity of the synthesized compounds follows as: F > E > D > C > B > A. The destructive effect of metal ions upon bacterial cell walls is responsible for enhanced activity of metal complexes as compared with ligand. Therefore, chelation reaction has a positive influence on biochemical potential of bioactive organic species. Attempting to change hydrophilicity and lipophilicity is likely to reduce cell solubility and permeability barriers. Furthermore, coordination modifies lipophilicity, which controls the rate of molecule entry into the cell, allowing the metal complex to grow more operative than the free ligand.

Antifungal activity

In vitro antifungal studies were performed for ligand and metal complexes against two different fungal strains namely *Candida albicans* and *Aspergillus niger*. It is apparent from the studies that, antifungal activity has been improved for the ligand after co-ordination with the metal.

The antifungal activities of the ligand and transition metal complexes were screened by agar well diffusion and minimum inhibitory concentration (MICs) method and the results are represented by Fig. 9. Fucanazole was used as a standard drug and the resulted zone of inhibition is depicted in Table 3. The synthesized transition metal complexes **(B-F)** were effectively examined for their *in vitro* studies against *Candida albicans* and *Aspergillus niger*. The minimum inhibitory concentration of the tested transition metal complexes **(B-F)** against fungal strains ranged from 10-60 µg/mL. It is noteworthy that the complexes **a**, **b** and **c** were found to be moderately active while the complexes D and F showed significant activity against *Candida albicans* strain. Besides, the complexes *E*, showed better anti-fungal activity against *Candida albican.*

With respect to *Aspergillus niger* all the synthesized complexes displayed moderate to significant antifungal activity. It is noteworthy that growth inhibition rate of fungi *Candida albicans* is higher in relation to *Aspergillus niger* with respect to all the compounds under study. It has been proposed that the ligands with the N and O donor system may have suppressed enzyme synthesis, because enzymes that need free hydroxyl groups for action tend to be

Table 3 — Antifungal activity of Schiff bases and transition metal complexes (4a-g) with zone inhibition (in mm).

Complexes	*Candida albicans*	*Aspergillus niger*
HL	9	10
4a	13	13
4b	14	12
4c	15	12
4d	12	10
4e	13	14
4f	15	13
4g	14	12
Control	22	20

Reference drug: Fucanazole

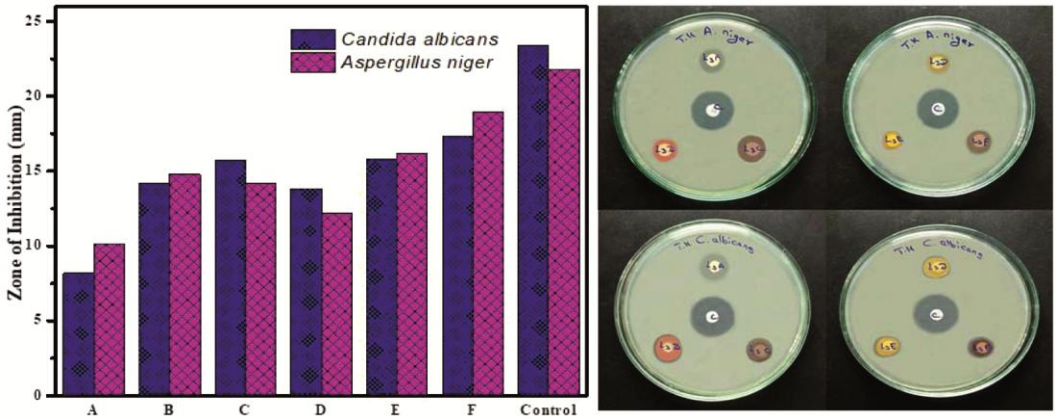

Fig. 9 — The antifungal activities of the ligand and metal complexes were screened by agar well diffusion and minimum inhibitory concentration (MICs) method.

more resistant to complex ion deactivation. By interacting with the -OH groups of certain cell enzymes, the complexes enhance their passage through the lipid layer of spore membranes to the site of action, finally killing them. The impermeability of the cell determines how effectively various biocidal agents work against various species.

DPPH radical scavenging assay

Antioxidant defenses against the DPPH radical, which is a stable free radical having a tendency to accept hydrogen ion or an electron to develop a stable molecule depends greatly on their capability to contribute hydrogen. One of the main causes of damage to the internal organs and tissues is, as well as causing various diseases such as diabetes, kidney injury, cancer, irritability, and so on, is free radical or oxidative damage. As a result, antioxidant agent is crucial for boosting by avoiding the production of free radicals in the internal organs. The findings of the antioxidant free-radical quenching activity were displayed in Fig. 10.

The reduction in its absorbance at 517 nm caused by antioxidants is used to calculate the decrease in the DPPH radical's capacity. From the results it could be inferred that antioxidant activity of complex F is greater than that of ligand as well as other metal complexes under study. This behavior could be explained by the fact that proton dissociation that form the complex F is more facile in relation to other. This information reveals that the metal ion exhibits nearly identical free radical mobility when compared to standard, demonstrating that the ligand enhances its function based on cooperation with metal ions and to guard the body against numerous ailments. The IC_{50} values of L and complex **F** were determined as 0.258 and 0.453 (mg/mL) respectively. The findings demonstrate that the formation of metal-ligand coordination clearly increases scavenger activity, and that the kind of metal ions also influences this capacity. Due to the chelation of organic molecules to metal ions, complexes have a significant capacity for radical scavenging, and metal ions have different and selective effects on radical scavengers in biological systems.

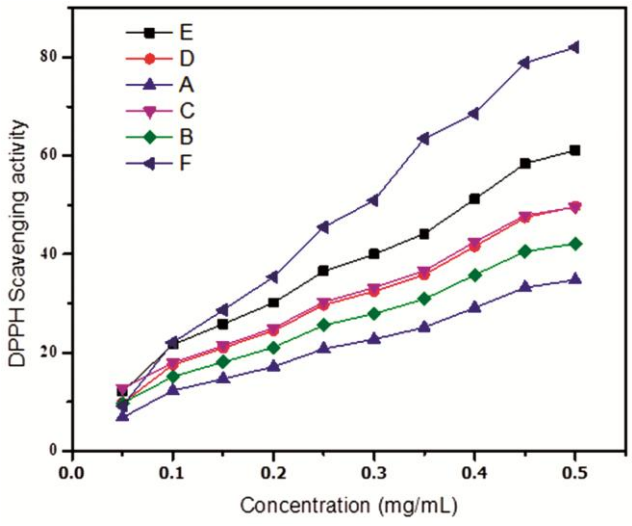

Fig. 10 — The DPPH radical scavenging activity of ligand and metal complex **F**.

Molecular Docking studies

The binding affinity of both ligands and active residues present in the binding cavity of protein is studied through molecular docking studies. The active residues located in the binding pocket of protein was determined by fixing the grid with 3Å in size with respect of native ligands of both protein Estrogen receptor alpha. As per the formation of better interaction, the docking score was considered. Based on the least docking score, the synthesized compound was listed Table 4. Of the six different synthesized metal complexes and ligand were tested, based on the lesser binding energy there are three out of seven of the synthesized compounds that falls within the threshold (–6 kcal/mol) against Estrogen receptor alpha respectively. In particular, the docking score was ranged between –8.9 kcal/mol to –7.8 kcal/mol (Fig. 11). Among the tested complexes, complex **F** produces least docking score (–8.9 kcal/mol) against Estrogen receptor alpha complex. Around eleven active contacts were observed between complex d and active residues of Estrogen receptor alpha. The second least docking score was observed for ***c*** (–8.7 kcal/mol) followed by other metal complex.

We have also examined by molecular docking to determine the extent of binding affinity of all the synthesized metal complexes and ligand. The active residues located in the binding pocket of protein were determined by fixing the grid with 3Å in size with respect of native ligands of both protein Estrogen receptor alpha. The metal complexes were performed with respect of native ligand of both protein Estrogen receptor alpha. Among the metal complexes and ligand, the molecular docking of complex **F** has least docking score (–8.9 kcal/mol) against Estrogen receptor alpha. The low value of the binding energy exhibit better effective binding affinity between Estrogen receptor alpha and **L**. It is bound to the

Table 4 — The Molecular Docking Parameter for sysnthesised Ligand & Metal Complexes with Protein Estrogen receptor alpha

Compd Name	Interactions	Distance	Category	Types of bond	From	From Chemistry	To	To Chemistry
Ligand	TYR526 - UNK0	4.6229	Hydrophobic	Pi-Pi Stacked	TYR526	Pi-Orbitals	UNK0	Pi-Orbitals
	TYR526 - UNK0	3.9222	Hydrophobic	Pi-Pi Stacked	TYR526	Pi-Orbitals	UNK0	Pi-Orbitals
	UNK0 - LYS529	5.3464	Hydrophobic	Pi-Alkyl	UNK0	Pi-Orbitals	LYS529	Alkyl
	UNK0 - LEU525	5.0083	Hydrophobic	Pi-Alkyl	UNK0	Pi-Orbitals	LEU525	Alkyl
	UNK0 - LYS529	5.4352	Hydrophobic	Pi-Alkyl	UNK0	Pi-Orbitals	LYS529	Alkyl
4a	UNK0:Mn - GLU380:OE2	2.1215	Other	Metal-Acceptor	UNK0:Mn	Metal	GLU380:OE2	H-Acceptor
	UNK0:Mn - UNK0:O	1.7916	Other	Metal-Acceptor	UNK0:Mn	Metal	UNK0:O	H-Acceptor
	UNK0:Mn - UNK0:O	1.7928	Other	Metal-Acceptor	UNK0:Mn	Metal	UNK0:O	H-Acceptor
	GLU380:OE1 -UNK0	3.8821	Electrostatic	Pi-Anion	GLU380:OE1	Negative	UNK0	Pi-Orbitals
	LEU536:CB - UNK0	3.7236	Hydrophobic	Pi-Sigma	LEU536:CB	C-H	UNK0	Pi-Orbitals
	MET522:SD:B - UNK0	5.8497	Other	Pi-Sulfur	MET522:SD:B	Sulfur	UNK0	Pi-Orbitals
	TYR537 - UNK0	5.1239	Hydrophobic	Pi-Pi Stacked	TYR537	Pi-Orbitals	UNK0	Pi-Orbitals
	TYR537 - UNK0	4.4828	Hydrophobic	Pi-Pi Stacked	TYR537	Pi-Orbitals	UNK0	Pi-Orbitals
	CYS381 - UNK0	4.5035	Hydrophobic	Alkyl	CYS381	Alkyl	UNK0	Alkyl
	UNK0 - LEU536	4.5912	Hydrophobic	Pi-Alkyl	UNK0	Pi-Orbitals	LEU536	Alkyl
4b	UNK0:Fe - GLU380:OE2	2.7121	Other	Metal-Acceptor	UNK0:Fe	Metal	GLU380:OE2	H-Acceptor
	UNK0:Fe - UNK0:O	1.8011	Other	Metal-Acceptor	UNK0:Fe	Metal	UNK0:O	H-Acceptor
	UNK0:Fe - UNK0:O	1.7926	Other	Metal-Acceptor	UNK0:Fe	Metal	UNK0:O	H-Acceptor
	GLU380:OE1 - UNK0	3.7484	Electrostatic	Pi-Anion	GLU380:OE1	Negative	UNK0	Pi-Orbitals
	GLU380:OE2 - UNK0	4.1474	Electrostatic	Pi-Anion	GLU380:OE2	Negative	UNK0	Pi-Orbitals
	LEU536:CB - UNK0	3.7547	Hydrophobic	Pi-Sigma	LEU536:CB	C-H	UNK0	Pi-Orbitals
	LEU536:CD1 - UNK0	3.9443	Hydrophobic	Pi-Sigma	LEU536:CD1	C-H	UNK0	Pi-Orbitals
	TYR537 - UNK0	5.0906	Hydrophobic	Pi-Pi Stacked	TYR537	Pi-Orbitals	UNK0	Pi-Orbitals
	TYR537 - UNK0	4.3297	Hydrophobic	Pi-Pi Stacked	TYR537	Pi-Orbitals	UNK0	Pi-Orbitals
	CYS381 - UNK0	4.1547	Hydrophobic	Alkyl	CYS381	Alkyl	UNK0	Alkyl
4c	UNK0:Co - GLU380:OE2	2.6480	Other	Metal-Acceptor	UNK0:Co	Metal	GLU380:OE2	H-Acceptor
	UNK0:Co - UNK0:O	1.7188	Other	Metal-Acceptor	UNK0:Co	Metal	UNK0:O	H-Acceptor
	UNK0:Co - UNK0:O	1.7258	Other	Metal-Acceptor	UNK0:Co	Metal	UNK0:O	H-Acceptor
	GLU380:OE1 - UNK0	3.7676	Electrostatic	Pi-Anion	GLU380:OE1	Negative	UNK0	Pi-Orbitals
	GLU380:OE2 - UNK0	4.1862	Electrostatic	Pi-Anion	GLU380:OE2	Negative	UNK0	Pi-Orbitals
	LEU536:HN - UNK0	3.2296	Hydrogen Bond	Pi-Donor Hydrogen Bond	LEU536:HN	H-Donor	UNK0	Pi-Orbitals
	LEU536:CB - UNK0	3.5934	Hydrophobic	Pi-Sigma	LEU536:CB	C-H	UNK0	Pi-Orbitals
	LEU536:CD1 - UNK0	3.9957	Hydrophobic	Pi-Sigma	LEU536:CD1	C-H	UNK0	Pi-Orbitals
	TYR537 - UNK0	5.1376	Hydrophobic	Pi-Pi Stacked	TYR537	Pi-Orbitals	UNK0	Pi-Orbitals
	TYR537 - UNK0	4.3202	Hydrophobic	Pi-Pi Stacked	TYR537	Pi-Orbitals	UNK0	Pi-Orbitals
	CYS381 - UNK0	4.4482	Hydrophobic	Alkyl	CYS381	Alkyl	UNK0	Alkyl
4d	UNK0:Ni - GLU380:OE2	2.8755	Other	Metal-Acceptor	UNK0:Ni	Metal	GLU380:OE2	H-Acceptor
	UNK0:Ni - UNK0:O	2.0016	Other	Metal-Acceptor	UNK0:Ni	Metal	UNK0:O	H-Acceptor
	UNK0:Ni - UNK0:O	2.0179	Other	Metal-Acceptor	UNK0:Ni	Metal	UNK0:O	H-Acceptor
	GLU380:OE1 - UNK0	3.8137	Electrostatic	Pi-Anion	GLU380:OE1	Negative	UNK0	Pi-Orbitals
	GLU380:OE2 - UNK0	4.3592	Electrostatic	Pi-Anion	GLU380:OE2	Negative	UNK0	Pi-Orbitals
	LEU536:HN - UNK0	3.3505	Hydrogen Bond	Pi-Donor Hydrogen Bond	LEU536:HN	H-Donor	UNK0	Pi-Orbitals
	LEU536:CB - UNK0	3.6176	Hydrophobic	Pi-Sigma	LEU536:CB	C-H	UNK0	Pi-Orbitals
	LEU536:CD1 - UNK0	3.8948	Hydrophobic	Pi-Sigma	LEU536:CD1	C-H	UNK0	Pi-Orbitals
	TYR537 - UNK0	5.0427	Hydrophobic	Pi-Pi Stacked	TYR537	Pi-Orbitals	UNK0	Pi-Orbitals
	TYR537 - UNK0	4.2981	Hydrophobic	Pi-Pi Stacked	TYR537	Pi-Orbitals	UNK0	Pi-Orbitals
	CYS381 - UNK0	4.5586	Hydrophobic	Alkyl	CYS381	Alkyl	UNK0	Alkyl

(*Contd.*)

Table 4 — The Molecular Docking Parameter for sysnthesised Ligand & Metal Complexes with Protein Estrogen receptor alpha (*Contd.*)

Compd Name	Interactions	Distance	Category	Types of bond	From	From Chemistry	To	To Chemistry
4e	UNK0:Cu - UNK0:O	1.4955	Other	Metal-Acceptor	UNK0:Cu	Metal	UNK0:O	H-Acceptor
	UNK0:Cu - UNK0:O	1.5061	Other	Metal-Acceptor	UNK0:Cu	Metal	UNK0:O	H-Acceptor
	TYR526 - UNK0	4.6909	Hydrophobic	Pi-Pi T-shaped	TYR526	Pi-Orbitals	UNK0	Pi-Orbitals
	UNK0 - PRO535	4.1195	Hydrophobic	Alkyl	UNK0	Alkyl	PRO535	Alkyl
	UNK0 - MET522	5.3754	Hydrophobic	Pi-Alkyl	UNK0	Pi-Orbitals	MET522	Alkyl
	UNK0 - LEU525	4.6693	Hydrophobic	Pi-Alkyl	UNK0	Pi-Orbitals	LEU525	Alkyl
4f	UNK0:Zn - GLU380:OE2	5.5210	Electrostatic	Attractive Charge	UNK0:Zn	Positive	GLU380:OE2	Negative
	UNK0:Zn - UNK0:O	1.7109	Other	Metal-Acceptor	UNK0:Zn	Metal	UNK0:O	H-Acceptor
	UNK0:Zn - UNK0:O	1.7141	Other	Metal-Acceptor	UNK0:Zn	Metal	UNK0:O	H-Acceptor
	MET522:SD - UNK0	5.1086	Other	Pi-Sulfur	MET522:SD	Sulfur	UNK0	Pi-Orbitals
	TYR526 - UNK0	4.6286	Hydrophobic	Pi-Pi Stacked	TYR526	Pi-Orbitals	UNK0	Pi-Orbitals
	TYR526 - UNK0	4.0862	Hydrophobic	Pi-Pi Stacked	TYR526	Pi-Orbitals	UNK0	Pi-Orbitals
	UNK0 - PRO535	5.2818	Hydrophobic	Alkyl	UNK0	Alkyl	PRO535	Alkyl
	UNK0 - LEU536	4.4121	Hydrophobic	Pi-Alkyl	UNK0	Pi-Orbitals	LEU536	Alkyl
	UNK0 - LEU525	5.1742	Hydrophobic	Pi-Alkyl	UNK0	Pi-Orbitals	LEU525	Alkyl
	UNK0 - LEU536	5.4438	Hydrophobic	Pi-Alkyl	UNK0	Pi-Orbitals	LEU536	Alkyl
4g	UNK0:Cd - UNK0:O	1.9207	Other	Metal-Acceptor	UNK0:Cd	Metal	UNK0:O	H-Acceptor
	UNK0:Cd - UNK0:O	1.9272	Other	Metal-Acceptor	UNK0:Cd	Metal	UNK0:O	H-Acceptor
	MET522:SD - UNK0	5.8079	Other	Pi-Sulfur	MET522:SD	Sulfur	UNK0	Pi-Orbitals
	PRO535 - UNK0	4.5484	Hydrophobic	Alkyl	PRO535	Alkyl	UNK0	Alkyl
	UNK0 - LYS529	4.7104	Hydrophobic	Pi-Alkyl	UNK0	Pi-Orbitals	LYS529	Alkyl
	UNK0 - VAL533	5.4805	Hydrophobic	Pi-Alkyl	UNK0	Pi-Orbitals	VAL533	Alkyl
	UNK0 - LEU525	4.7268	Hydrophobic	Pi-Alkyl	UNK0	Pi-Orbitals	LEU525	Alkyl

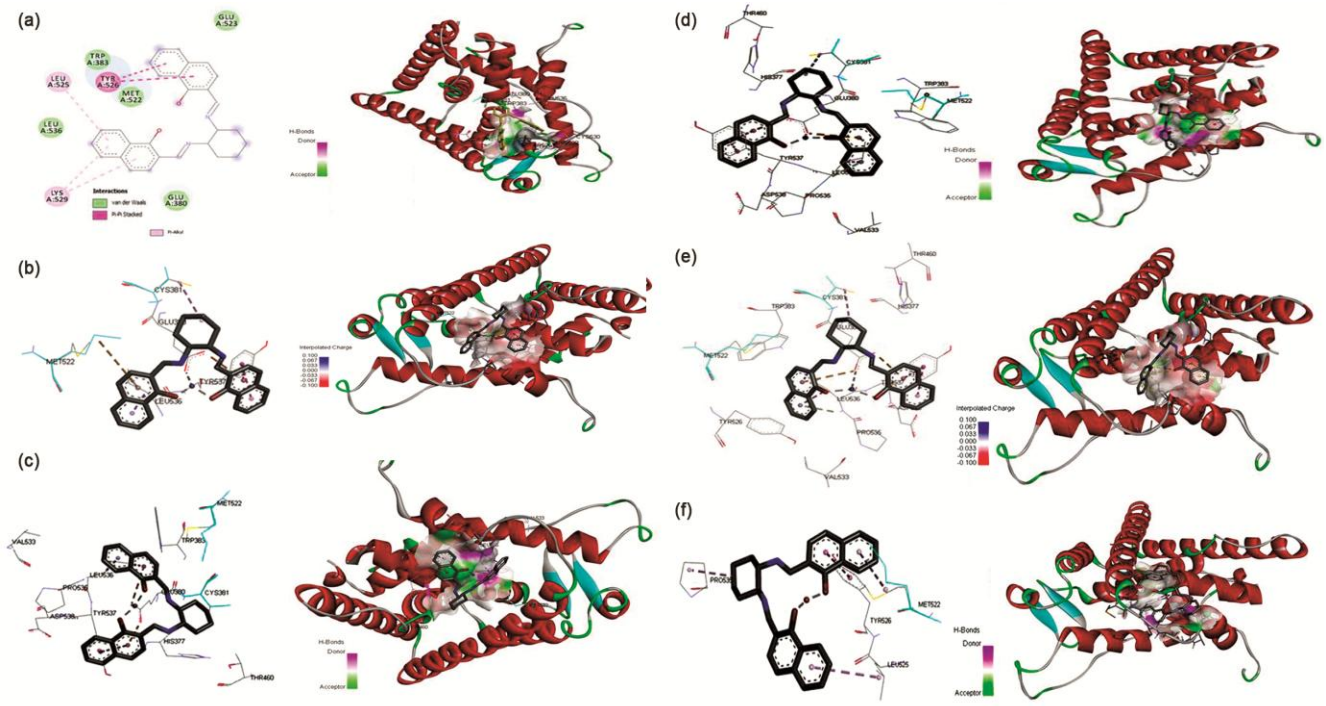

Fig. 11 — The molecular docking interaction images of ligand and metal complexes.

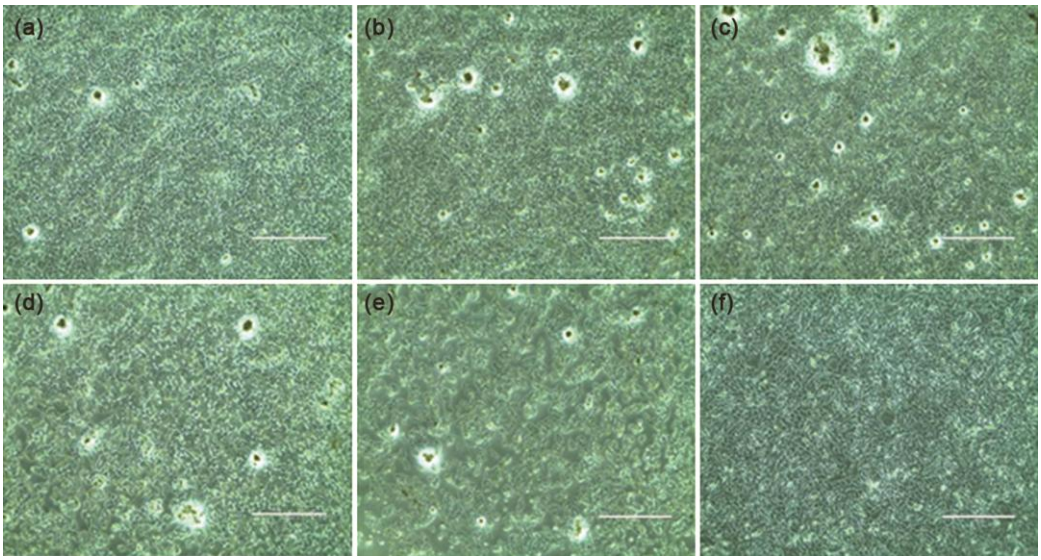

Fig. 12 — The MTT assay exhibited concentration dependent reduction in cell viability for complex **F** against MCF- 7cell line.

active residues by showing eight alkyl bonds (NUK0, A: MEI522, A: PRO535 and UNK0: Br) (Table 4) Around eight active contacts were observed between A and active residues of Estrogen receptor alpha. Next, we have observed the second least docking score for complex **B** and **C** (–9.8 kcal/mol). The present study proved that, **F** provided better results with Estrogen receptor alpha when compared with other metal complexes. This is due to good binding ability of complex F and also the docked images are shown in Fig. 11.

Anticancer studies

The creation of transition metal-based pharmaceuticals has shown to be a potential method to discover a pharmacological solution for the treatment of several disorders, including cancer. The MTT assay for compound F against the MCF-7 cell line demonstrated a concentration-dependent reduction in cell viability, as shown in Fig. 12. FEM was applied to the cells in concentrations ranging from (25 g) to (150 g). After 24 hours of incubation, a strong anti-cancer activity against MCF-7 cells was discovered using the MTT colorimetric assay. The proliferative activity for cells was shown in Fig. 13 in a dose-dependent way. Complex **F** has an IC50 of 86.68 0.72 g/mL for MCF-7 cells. It was shown that complex **F** showed potential anticancer action against breast cancer cell lines based on the findings of the MTT experiment. For the treatment of breast cancer, the metal complex **F** may be utilized as an effective carrier.

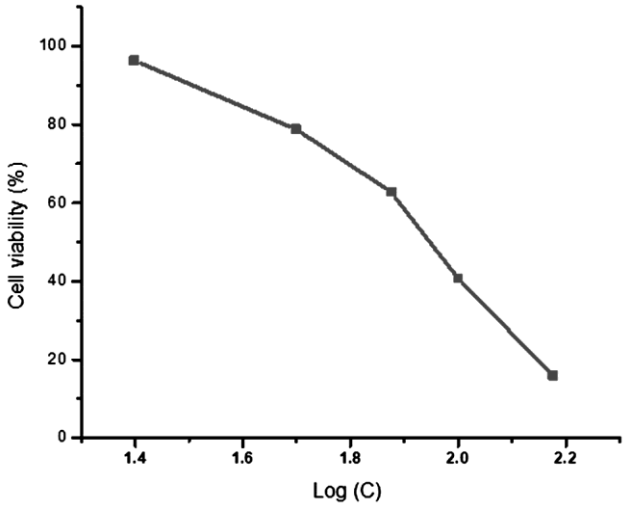

Fig. 13 — Plot for %inhibition with concentration of complex **F** in MTT assay using MCF-7 cells.

Conclusions

When ligands are made from bioactive substances, they acquire various physicochemical and pharmacological characteristics. Herein, we have successfully attempted to prepare 1-hydroxy naphthaldehyde based ligand and a series of transition metal complexes through a simple condensation reaction. Utilizing UV-Vis, FT-IR, NMR, elemental analysis, and ESI-MS spectral analysis, the materialization of the ligand is supported. The antimicrobial study was performed using both bacteria and fungi microorganisms. Both antimicrobial and antioxidant studies demonstrated

that Ni(II) complex exhibits superior activity. Besides, least binding score associated with this complex from molecular docking studies, well-proved that it is capable of forming efficient binding with biomolecules in relation to other metal complexes under study. The MCF-7 cancer cell lines were used in the anti-proliferative activity Ni(II) complex test, and the result showed an IC50 value of 103.1 (g/ml). Since, the exploration for more active low cost metal-based anticancer drugs with good selectivity and least side effects is the need of the hour, in this study, the procedure for making novel ligands and their matching metal complexes with a variety of metals from the periodic table was summarized, and their biological activity was examined. The reported investigation suggested that synthesized metal complexes that are prospective candidates for diverse biomedical, pharmaceutical and drug delivery applications that could fascinate the consideration of the scientific community.

Declaration of competing interest

All authors declare no conflict of interest.

References

1 Suganthy P K, Prabhu R N & Sreedevi V S, *Tetrahedron Lett,* 54 (2013) 5695.
2 Verma P R, Mandal S, Gupta P & Mukhopadhyay B, *Tetrahedron Lett,* 54 (2013) 4914.
3 Prabhu R N & Ramesh R, *Tetrahedron Lett,* 53 (2012) 5961.
4 Datta S, Seth D K, Gangopadhyay S, Karmakar P & Bhattacharya S, *Inorg Chim Acta,* 392 (2012) 118.
5 Lobana T S, Bawa G, Butcher R J, Liaw B J & Liu C W, *Polyhedron,* 25 (2006) 2897.
6 Corhnelissen J P, Van Diemen J H, Groeneveld L R, Haasnoot J G, Spek A L & Reedisk J, *Inorg Chem,* 31 (1992) 198.
7 Vila J M, Pereira T, Ortigueira J M, Lopez-Torres M, Castineiras A, Lata D, Fernandez J J & Fernandez A, *J Organomet Chem,* 556 (1998) 21.
8 Vila J M, Pereira M T, Ortigueira J M, Grana M, Lata D, Suarez A, Fernandez A, Lopez-Torres M & Adams H, *J Chem Soc Dalton Trans,* (1999) 4193.
9 Vigato P A & Tamburani S, *Coord Chem Rev,* 248 (2004) 1717.
10 Barboiu C T, Luca M, Pop C, Brewster E & Dinculescu M E, *Eur J Med Chem,* 3 (1996) 597.
11 Radha V P, Kirubavathy S J & Chitra S, *J Mol Struct,* 1165 (2018) 246.
12 Kareem, Khan M S, Nami S A A, Bhat S A, Mirza A U & Nishat N, *J Mol Struct,* 1167 (2018) 261.
13 Zhao F, Wang W, Lu W, Xu L, Yang S, Cai X M, Zhou M, Lei M, Ma M, Xu H J & Cao F, *Eur J Med Chem,* 146 (2018) 451.
14 Iftikhar B, Javed K, Khan M S U, Akhter Z, Mirza B & Mckee V, *J Mol Struct,* 1155 (2018) 337.
15 Alam M S, Choi J H & Lee D U, *Bioorg Med Chem,* 20 (2012) 4103.
16 Kumar K S, Ganguly S, Veerasamy R & Clercq E D, *Eur J Med Chem,* 45 (2010) 5474.
17 Desai S B, Desai P B & Desai K R, *Heterocycl Commun,* 7 (2001) 83.
18 Sarkar S, Nag S K, Chattopadhyay A P, Dey K, Islam S M, Sarkar A & Sarkar S, *J Mol Struct,* 1160 (2018) 9.
19 Ayoub M A, Abd-Elnasser E H, Ahmed M A & Rizk M G, *J Mol Str,* 1163 (2018) 379.
20 Egekenze R N, Gultneh Y, Butcher R, *Inorg Chim Acta,* 478 (2018) 232.
21 Gaur S, *Asian J Chem,* 15 (2003) 250.
22 Gemi M J, Biles C, Keiser B J, Poppe S M, Swaney S M, Tarapley W G, Romeso D L & Yage Y, *J Med Chem,* 43 (2000) 1034.
23 Elzahany E A, Hegab K H, Khalil S K H, Youssef N S, *Aust J Basic Appl Sci,* 2 (2008) 210.
24 Morad F M, El-Ajaily M M, Ben Gweirif S, *J Sci Appl,* 1 (2007) 72.
25 Kshirsagar V S, Garade A C, Mane R B, Patil K R, Yamaguchi A , Shirai M, Rode C V, *Appl Catal A,* 370 (2009) 16.
26 Refat M S, El-Deen I M, Ibrahim H K, El-Ghool S, *Spectrochim Acta Part A Mol Biomol Spectrosc,* 65 (2006) 1208.
27 Brooker S, Iremonger S S & Plieger P G, *Polyhedron,* 22 (2003) 665.
28 Manimalathi S & Madheswari D, *Indian J Chem A,* 61 (2022) 965.
29 Priya J & Madheswari D, *J Biosci,* 47 (2022) 29.
30 Hong M, Yin H, Zhang X, Li C, Yue C & Cheng S, *J Organometallic Chem,* 724 (2013) 23.
31 Abbasi Z, Salehi M, Khaleghian A, Kubicki M, *J Mole Struc,* 1173 (2018) 213.
32 Qi J, Luo Y, Zhou Q, Su G, Zhang X, Nie X, Lv M, Li W, *J Mole Struc,* 1255 (2022) 132458.
33 Nagesh G Y, Mruthyunjayaswamy B H M, *J Mole Struc,* 1085 (2015) 198.
34 Ismael M, Abdel-Mawgoud A M, Mostafa Rabia K, Aly Abdou, *J Mol Liquids,* 330 (2021) 115611.
35 Mohanapriya S, Mumjitha M, Purna sai K, Raj V, *J Mech Behav Biomed Mater,* 63 (2016) 141.
36 Mohanapriya S & Raj V, *Mater Sci Engg C,* 86 (2018) 70.
37 Sangeetha T V, Mohanapriya S & Bhuvaneswari N, *Ind J Chem,* 60A (2021) 797.
38 Manimalathi S & Madheswari D, *Indian J Chem A,* 61 (2022) 965
39 Petros A M, Medek A, Nettesheim D G, Kim D H, Yoon H S, Swift K, Matayoshi T, Oltersdorf E D, Fesik S W, *Proc Natl Acad Sci,* 98 (2001) 3012.
40 Uppalapati S R, Kingston J J, Qureshi I A, Murali H S, Batra H V, *PLOS One,* 8 (2013) 82024.
41 Usha T, Goyal A K, Lubna S, Prashanth H, Mohan T M, Pande V, Middha S K, *Asian. Pac J Cancer Prev,* 15 (2014) 10345.